# Recent near-Earth supernovae probed by global deposition of interstellar radioactive [60]Fe

**A. Wallner**[1], **J. Feige**[2], **N. Kinoshita**[3], **M. Paul**[4], **L.K. Fifield**[1], **R. Golser**[2], **M. Honda**[5], **U. Linnemann**[6], **H. Matsuzaki**[7], **S. Merchel**[8], **G. Rugel**[8], **S.G. Tims**[1], **P. Steier**[2], **T. Yamagata**[9], and **S.R. Winkler**[2]

[1]Department of Nuclear Physics, Research School of Physics and Engineering, Australian National University, Canberra, ACT 2601, Australia

[2]University of Vienna, Faculty of Physics — Isotope Research, VERA Laboratory, Währinger Straße 17, 1090 Vienna, Austria

[3]Institute of Technology, Shimizu Corporation, Tokyo 135-8530, Japan

[4]Racah Institute of Physics, The Hebrew University of Jerusalem, Jerusalem 91904, Israel

[5]Graduate School of Pure and Applied Sciences, University of Tsukuba, Ibaraki 305-8577, Japan

[6]Senckenberg Collections of Natural History Dresden, GeoPlasmaLab, Königsbrücker Landstraße 159, Dresden 01109, Germany

[7]MALT (Micro Analysis Laboratory, Tandem accelerator), The University Museum, The University of Tokyo, Tokyo 113-0032, Japan

[8]Helmholtz-Zentrum Dresden-Rossendorf (HZDR), Helmholtz Institute for Resource Technology, 01328 Dresden, Germany

[9]Graduate School of Integrated Basic Sciences, Nihon University, Tokyo 156-8550, Japan

## Abstract

The rate of supernovae (SNe) in our local galactic neighborhood within a distance of ~100 parsec from Earth (1 parsec (pc)=3.26 light years) is estimated at 1 SN every 2-4 million years (Myr), based on the total SN-rate in the Milky Way ($2.0 \pm 0.7$ per century[1,2]). Recent massive-star and SN activity in Earth's vicinity may be evidenced by traces of radionuclides with half-lives $t_{1/2}$ 100 Myr[3-6], if trapped in interstellar dust grains that penetrate the Solar System (SS). One such radionuclide is [60]Fe ($t_{1/2}$=2.6 Myr)[7,8] which is ejected in supernova explosions and winds from

massive stars[1,2,9]. Here we report that the $^{60}$Fe signal observed previously in deep-sea crusts[10,11], is global, extended in time and of interstellar origin from multiple events. Deep-sea archives from all major oceans were analyzed for $^{60}$Fe deposition via accretion of interstellar dust particles. Our results, based on $^{60}$Fe atom-counting at state-of-the-art sensitivity[8], reveal $^{60}$Fe interstellar influxes onto Earth 1.7–3.2 Myr and 6.5–8.7 Myr ago. The measured signal implies that a few percent of fresh $^{60}$Fe was captured in dust and deposited on Earth. Our findings indicate multiple supernova and massive-star events during the last ~10 Myr at nearby distances 100 pc.

The density and temperature distribution of the interstellar medium (ISM) is highly variable, with typical substructures of ~50–150 pc (superbubbles) having life-times of some 10 Myr. Several SN explosions over the last ~14 Myr shaped the present structure of the local superbubble (LB)[12-14]. The SS, now embedded in the LB, is expected to have faced fronts of SN ejecta and accumulated material from massive stars. To enter the SS, any material from the ISM must be condensed into larger dust grains to avoid being deflected away by the solar wind and interplanetary magnetic field[3,10,11]. ISM dust particles were indeed identified at Earth orbit[15] and may accumulate on Earth in archives such as deep-sea sediments and ferromanganese (FeMn) crusts and nodules which retain time information over millions of years. $^{60}$Fe as well as $^{26}$Al ($t_{1/2}$=0.71 Myr) are observed[1,9] in the ISM as a result of many SNe and emission from massive stars. Direct detection of 'live' radionuclides[3-5,10,11] on Earth would provide insight into recent and nearby nucleosynthesis in massive stars[14,16,17], dust formation and transport into the SS. Extraterrestrial $^{60}$Fe was in fact already observed in FeMn crusts in pioneering studies at TU Munich[10,11], and interpreted as being of SN[10,11,18] or (micro)meteoritic origin[19,20].

In the present work, the $^{60}$Fe contents of three different deep-sea archives (four sediment cores, two FeMn-crusts and two FeMn-nodules) recovered from the Indian, Pacific and Atlantic Oceans respectively (Supplementary Figure S1) were determined. All were dated via their $^{10}$Be ($t_{1/2}$=1.39 Myr) content, complemented by $^{26}$Al for the sediments[21]. All radionuclides ($^{60}$Fe, $^{26}$Al and $^{10}$Be) were counted using accelerator mass spectrometry (AMS) (Supplementary Information). The sediment cores provided a record from 1.7-3.2 Myr BP (before present) with a time resolution of <30 kyr, bracketed by recent and ~5-7 Myr old samples. Pacific 'Crust-1' extends from present to 10.9 Myr with ~2.2 Myr time resolution and 'Crust-2' from 1.2–7 Myr BP (~100 kyr resolution). Two nodules covered 5.4 Myr BP (~2 Myr resolution).

In the sediment, 288 $^{60}$Fe-events were registered for the time period 1.71-3.18 Myr (45 individual samples) with a mean isotopic ratio $^{60}$Fe/Fe=(1.79±0.10)×$10^{-15}$, a factor of ~40 above the measurement background of (0.042±0.015)×$10^{-15}$. None of the recent or old sediment samples show evidence for $^{60}$Fe above background (3 $^{60}$Fe-events). The first two layers in Crust-1 gave $^{60}$Fe-signals 4σ and 7σ above background; layers 3 and 5 are close to the measurement background, but layer 4, which spans the period 6.5-8.7 Myr, has a significantly higher ratio (~4σ above background, Table 2). For Crust-2 a clear $^{60}$Fe-signal was also found at <3.5 Myr. The nodules support this finding (Table 3, Supplementary Tables S3-S5).

In summary, two clear $^{60}$Fe signals with a total of 538 $^{60}$Fe-events were observed. In the sediments, the signal covers the time period 1.7–3.2 Myr. In the crusts, $^{60}$Fe is found up to 3.5 and ~4 Myr, with a second influx between 6.5 and 8.7 Myr. The nodules confirm the presence of $^{60}$Fe at <3.3 Myr. No $^{60}$Fe signal is found in recent (<0.2 Myr) or older ( 5 Myr) sediments and nodules, or in crusts between 4.4–6.5 and 8.7–10.9 Myr.

Between 1.7 and 3.1 Myr, the $^{60}$Fe deposition rate into the sediments was ~11–35 $^{60}$Fe atoms·cm$^{-2}$yr$^{-1}$ (300-kyr averages), whereas incorporation rates into crust material were significantly lower at 1–2 atoms·cm$^{-2}$·yr$^{-1}$ (Figure 1, all data are decay-corrected). This suggests an incorporation-efficiency into Crust-1 and Crust-2 of 17% and 7%, respectively. The deposition in the 1.5-Myr interval covered by the signal in the sediment is $(35\pm2)\times10^6$ atoms·cm$^{-2}$. For the second $^{60}$Fe signal (6.5-8.7 Myr, Crust-1, 17% incorporation) it is $(21\pm6)\times10^6$ atoms·cm$^{-2}$ (Tables 2-3).

Although the 1.5 Myr time-spread of $^{60}$Fe influx measured in the present work exceeds the ~0.8 Myr previously reported for crust 237KD[11,18], the two time profiles are not inconsistent given the lower counting statistics and signal-to-background in Ref. 11. Furthermore, the marginally positive result for the same time period for an Atlantic sediment[18] is consistent with our data, considering their higher sedimentation rates and stable Fe-contents. $^{60}$Fe has also been reported in lunar material, though without time information[22] and recently in Pacific sediments[23].

Clearly, our data are incompatible with a constant $^{60}$Fe production or deposition. A terrestrial origin can be ruled out, because there is no suitable target for cosmic-ray induced production and anthropogenic input would be concentrated in the surface layer. Since $^{60}$Fe was found in each of the major oceans, it is reasonable to assume a uniform global distribution. A micro-meteoritic or meteoritic origin can be excluded, since the measured cosmic-dust flux is 400 times lower than would be required (Supplementary Information and Figure S6). Similarly a hypothetical break-up of a single object, comparable to the asteroid invoked in relation to the K/T event 65 Myr ago, would have delivered 4,500 times less $^{60}$Fe.

We assume that the extraterrestrial $^{60}$Fe flux through Earth's cross-section is homogenously distributed over Earth's surface. Thus, the measured mean deposition of ~24.5 atoms·cm$^{-2}$yr$^{-1}$ (1.7–3.2 Myr signal) corresponds to a $^{60}$Fe-flux of 98 atoms·cm$^{-2}$yr$^{-1}$ into the inner SS or integrated over 1.5 Myr to an $^{60}$Fe-fluence of $(1.46\pm0.15)\times10^8$ atoms·cm$^{-2}$ at Earth orbit; the fluence for the older event is $(1.2\pm0.4)\times10^8$ atoms·cm$^{-2}$. Interstellar grains, filtered by the SS in size to an average of ~0.5 μm, were detected by space missions[15], suggesting that $(6\pm3)$% ($\varepsilon_{dust}$) in mass of ISM dust reaches the inner SS[6]. These grains follow the flow velocity of the ISM. Assuming the $^{60}$Fe-loaded grains follow the same mass-distribution as determined for ISM grains at Earth orbit, we deduce an interstellar $^{60}$Fe-concentration in dust of $(2.8\pm1.4)\times10^{-11}$ $^{60}$Fe atoms·cm$^{-3}$ for 1.7-3.2 Myr and integrated over the full period of 11 Myr an average concentration of ~$(5\text{-}15)\times10^{-12}$ atoms·cm$^{-3}$. Observations of $^{60}$Fe-decay[1,9] and nucleosynthesis models[2] suggest an average Galaxy concentration of ~$6\times10^{-12}$ $^{60}$Fe atoms·cm$^{-3}$ (Supplementary Information), in agreement with the 11-Myr local-data reported here.

[60]Fe is produced in massive stars[2,24-27] in their late phases, predominantly just before SN-explosions, and then ejected into space. (Super)AGB stars also produce and eject [60]Fe through their stellar winds during ~50 kyr, leading to a time profile similar to SNe; however, their contribution to the galactic [60]Fe inventory is small[28].

Models suggest a travel time of ~200 kyr with a time spread of ~100–400 kyr[5] for ejecta from a single SN at ~100pc distance. Our measured spread of ~1.5-Myr is inconsistent with the interpretation in terms of ejecta from a single SN (or AGB-star) moving across the SS (Supplementary Figure S6). It suggests multiple SN- and massive-star activities within the last ~10 Myr in Earth's vicinity and two distinct periods 1.7–3.2 and ~6.5–8.7 Myr BP. The recent time profile would be compatible with movement across the SS of ejecta in a series of SN-fronts in short succession within 1.5 Myr. This would, however, require a high SN-frequency (~2-3 SNe/Myr) since large fluctuations were not observed in the time profile. Alternatively, the ejecta containing the [60]Fe-bearing grains could have come to rest in the ambient ISM and diffused into volumes or clouds, that were then traversed by the SS[18].

The SS is currently embedded in a flow of ISM-material with interstellar grains moving parallel to the flow of neutral interstellar gas in local ISM clouds arguing for a common history or driver[29]. Such clouds were suggested as part of an expanding superbubble-shell driven by SNe and winds from massive stars[29,12-14]. Assuming the ejecta originate from a distance 70-100 pc (~limit of the LB) and [60]Fe is equally distributed into the outer shell of size 30 pc (distance representing 1.5 Myr travel), i.e. a spherical shell of mean radius 70-100 pc with a thickness of 30 pc, we deduce a total [60]Fe mass trapped in ISM dust of $(5–11) \times 10^{-5}$ solar masses $(M_\odot)$ in the shell volume. This number represents a lower limit as it reflects the fraction of [60]Fe condensed into dust without correction for radioactive decay and neglects the granularity of clumpy ejecta. Models predict core-collapse and electron-capture SN-nucleosynthesis yields for [60]Fe to be $(0.5–14) \times 10^{-5}$ $M_\odot$ for 8–25 $M_\odot$-stars[24-27,2], depending on the progenitor mass with large uncertainties in the nuclear-physics input. (Super)AGB stars produce $(0.003–1) \times 10^{-5}$ $M_\odot$ [60]Fe[28]. Our observed signals therefore favor SN events. The fraction of [60]Fe in dust can be roughly estimated by a comparison of our measured [60]Fe deposition with nucleosynthesis yields. Under these assumptions and assuming reasonable distances (20–100pc) ~0.4-9% of [60]Fe would be trapped in dust (Supplementary Information, Figures S7 and S8).

Comparing our data with a similar work for ISM-[244]Pu in sediments and crust samples[6] yields a [244]Pu/[60]Fe atom-ratio of $\sim 3 \times 10^{-5}$ or less during periods of elevated [60]Fe deposition over the last 10 Myr which agrees with the recently reported low [244]Pu SN-yields[6] (Supplementary Information).

Our broad and global [60]Fe-influx on Earth demonstrates recent (<10Myr) and wide-spread massive-star ejections in our near galactic neighborhood (<100pc), most likely from SN-explosions. Interestingly, the older event coincides with a strong increase in [3]He and temperature change ~8 Myr BP[30], while the more recent activity starting ~3 Myr BP occurred at the same time as Earth's temperature started to decrease during the Plio-Pleistocene transition.

## Supplementary Material

Refer to Web version on PubMed Central for supplementary material.

## Acknowledgements

## References

1. Diehl R. Nuclear astrophysics lessons from INTEGRAL. Rep. Prog. Phys. 2013; 76:026301. [PubMed: 23377195]

2. Timmes FX, Woosley SE. Gammy-ray line signals from $^{26}$Al and $^{60}$Fe in the Galaxies of the Local Group. Astrophys. J. 1997; 481:L81.

3. Ellis J, Fields BD, Schramm DN. Geological Isotope Anomalies as signatures of nearby supernovae. Astrophys. J. 1996; 470:1227–1236.

4. Korschinek G, Faestermann T, Knie K, Schmidt C. $^{60}$Fe, a Promising AMS Isotope for Many Applications. Radiocarbon. 1996; 38:68. abstract to AMS-conference AMS-7.

5. Fry BJ, Fields BD, Ellis JR. Astrophysical Shrapnel: Discriminating Among Extra-Earth Stellar Explosion Sources of Live Radioactive Isotopes. Astrophys. J. 2015; 800:71.

6. Wallner A, et al. Abundance of live $^{244}$Pu in deep-sea reservoirs on Earth points to rarity of actinide nucleosynthesis. Nature Communications. 2015; 6:5956.

7. Rugel G, et al. New measurement of the $^{60}$Fe half-life. Phys. Rev. Lett. 2009; 103:072502. [PubMed: 19792637]

8. Wallner A, et al. Settling the half-life of $^{60}$Fe – fundamental for a versatile astrophysical chronometer. Phys. Rev. Lett. 2015; 114:041101. [PubMed: 25679883]

9. Wang W, et al. SPI observations of the diffuse $^{60}$Fe emission in the Galaxy. Astron. Astrophys. 2007; 469:1005–1012.

10. Knie K, et al. Indication for Supernova Produced $^{60}$Fe Activity on Earth. Phys. Rev. Lett. 1999; 83:18–21.

11. Knie K, et al. $^{60}$Fe anomaly in a deep-sea manganese crust and implications for a nearby supernova source. Phys. Rev. Lett. 2004; 93:171103. [PubMed: 15525065]

12. Maiz-Apellaniz J. The Origin of the Local Bubble. Astrophys. J. 2001; 560:L83–L86.

13. Breitschwerdt D, de Avillez MA. The history and future of the Local and Loop I bubbles. Astron. Astrophys. 2006; 452:L1–L5.

14. Benitez N, Maiz-Apellaniz J, Canelles M. Evidence for Nearby Supernova Explosions. Phys. Rev. Lett. 2002; 88:081101. [PubMed: 11863949]

15. Mann I. Interstellar Dust in the Solar System. Annu. Rev. Astron. Astrophys. 2010; 48:173–203.

16. Beech M. The past, present and future supernova threat to Earth's biosphere. Astrophys. Space Science. 2011; 336:287–303.

17. Ruderman MA. Possible Consequences of Nearby Supernova Explosions for Atmospheric Ozone and Terrestrial Life. Science. 1974; 184:1079–1081. [PubMed: 17736193]

18. Fitoussi C, et al. Search for Supernova-Produced $^{60}$Fe in a Marine Sediment. Phys. Rev. Lett. 2008; 101:121101. [PubMed: 18851357]

19. Stuart FM, Lee MR. Micrometeorites and extraterrestrial He in a ferromanganese crust from the Pacific Ocean. Chemical Geology. 2012; 322–323:209–214.

20. Basu S, Stuart FM, Schnabel C, Klemm V. Galactic-cosmic-ray-produced $^3$He in a ferromanganese crust: any supernova $^{60}$Fe excess on Earth? Phys. Rev. Lett. 2007; 98:141103. [PubMed: 17501264]

21. Feige J, et al. AMS measurements of cosmogenic and supernova-ejected radionuclides in deep-sea sediment cores. EPJ Web of Conf. 2013; 63:03003.

22. Fimiani, L., et al. Evidence for Deposition of Interstellar Material on the Lunar Surface; Lunar and Planetary Science Conference, Lunar and Planetary Science Conference, Vol. 45; 2014. p. 1778

23. Ludwig, P. Search for $^{60}$Fe of supernova origin in Earth's microfossil record. TU Munich; 2015. PhD thesis

24. Woosley SE, Weaver TA. The evolution and explosion of massive stars. II. Explosive hydrodynamics and nucleosynthesis. The Astrophys. J. Suppl. Series. 1995; 101:181–235.

25. Rauscher T, Heger A, Hoffman RD, Woosley SE. Nucleosynthesis in Massive Stars with Improved Nuclear and Stellar Physics. Astrophys. J. 2002; 576:323–348.

26. Limongi M, Chieffi A. The Nucleosynthesis of $^{26}$Al and $^{60}$Fe in Solar Metallicity Stars Extending in Mass from 11 to 120 $M_O$: The Hydrostatic and Explosive Contributions. Astrophys. J. 2006; 647:483–500.

27. Wanajo S, Janka H-T, Müller B. Electron-Capture Supernovae as Sources of $^{60}$Fe. Astrophys. J. Lett. 2013; 774:L6.

28. Doherty CL, Gil-Pons P, Lau HHB, Lattanzio JC, Siess L. Super and massive AGB stars - II. Nucleosynthesis and yields - Z = 0.02, 0.008 and 0.004. Monthly Notices of the Royal Astronomical Society. 2014; 437:195–214.

29. Frisch PC, et al. The Galactic Environment of the Sun: Interstellar Material Inside and Outside of the Heliosphere. Space Sci. Rev. 2009; 146:235–273.

30. Farley KA, Vokrouhlicky D, Bottke WF, Nesvorny D. A late Miocene dust shower from the break-up of an asteroid in the main belt. Nature. 2006; 439:295–297. [PubMed: 16421563]
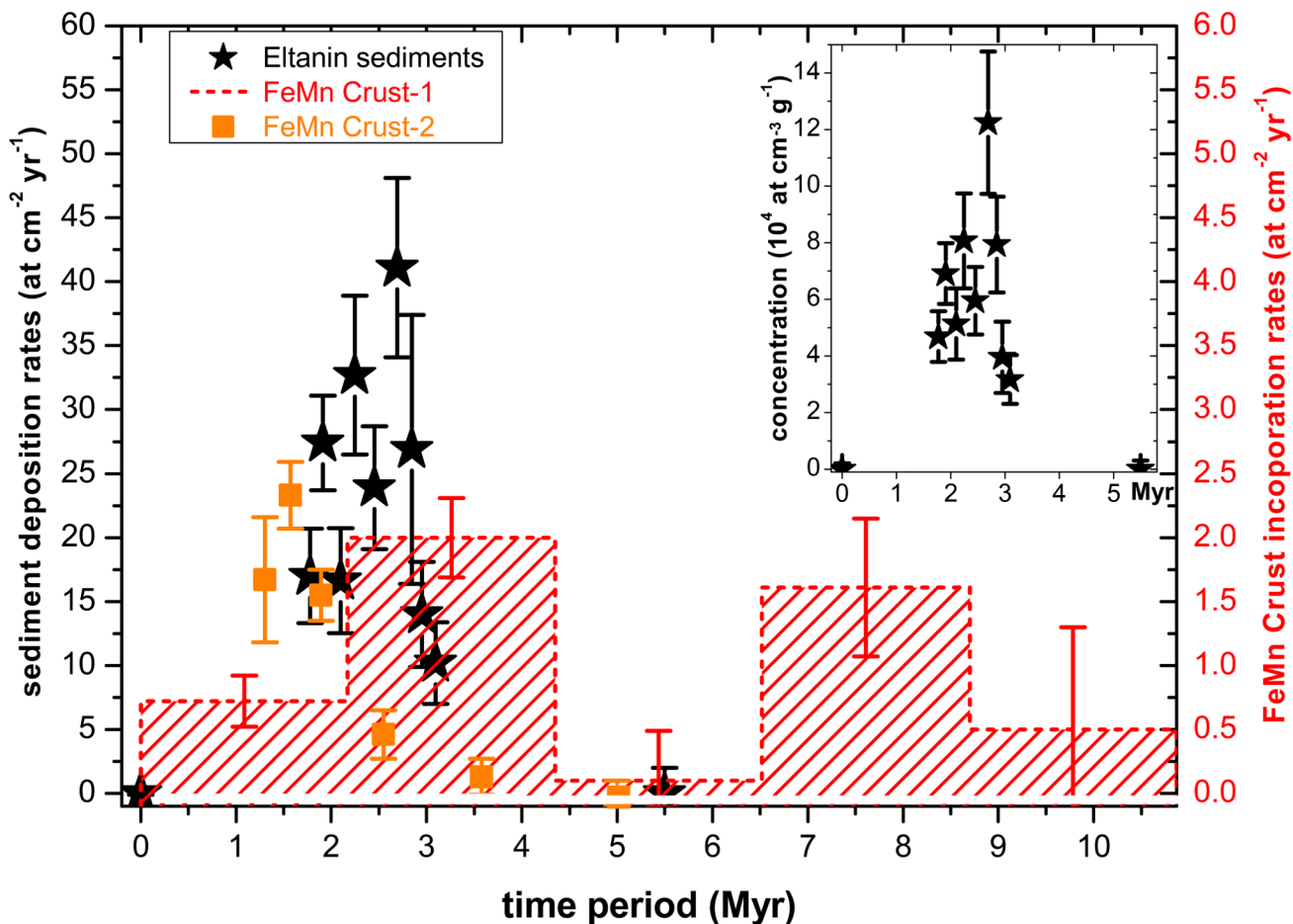
**Figure 1. Deposition rates for sediment (150 kyr averaged data) and incorporation rates for two crust samples**

$^{60}$Fe concentrations ($^{60}$Fe/g) for the sediment are given in the inset; they were on average $6.7 \times 10^4$ atoms/g between 1.7 and 3.2 Myr, but $260 \times 10^4$ atoms/g crust and $95 \times 10^4$ atoms/g nodule, reflecting the difference in growth rate and incorporation efficiency (see Supplement). The error bars ($1\sigma$) include all uncertainties and scale with decay correction, thus upper limits are becoming larger for older samples. The absolute ages for the sediment are uncertain by 0.1 Myr, but for the 5.5-Myr sediments ~1 Myr. Ages of Crust-1 are 0.3 and of Crust-2 0.5 Myr uncertain.

**Table 1**

**Averaged $^{60}$Fe/Fe atom ratios from AMS measurements at ANU**

52 sediment samples from four sediment cores (Eltanin) from the Indian Ocean were analyzed (individual data are listed in the Supplementary Information) as well as a series of blank samples (commercial iron).

| sediment cores | sediment samples | time period (Myr) | $^{60}$Fe counts detected | $^{60}$Fe/Fe ($10^{-15}$ at/at)[a] | $^{60}$Fe/Fe \|d.c. ($10^{-15}$ at/at)[b] | Fe conc. ($10^{-2}$ g g$^{-1}$)[c] | $^{60}$Fe conc. ($10^4$ at g$^{-1}$) | $^{60}$Fe-deposition rates (at cm$^{-2}$yr$^{-1}$) | $^{60}$Fe deposition ($10^6$ at·cm$^{-2}$ layer$^{-1}$)[d] |
|---|---|---|---|---|---|---|---|---|---|
| 45-21 / 50-02 | 5 | < 0.2 | 2 | 0.06±0.04 | 0.02±0.02 | 0.30±0.10 | <0.2 | <0.2 | -- |
| 49-53 / 45-21 | 14 | 1.71 – 2.0 | 123 | 1.67±0.15 | 2.52±0.23 | 0.23±0.01 | 6.0±0.6 | 22.8±2.3 | 6.5±0.7 |
| 49-53 / 45-21 / 50-02 | 11 | 2.0 – 2.3 | 51 | 1.51±0.21 | 2.48±0.35 | 0.24±0.01 | 6.7±1.0 | 24.8±3.6 | 7.4±1.1 |
| 49-53 / 45-21 / 50-02 | 7 | 2.3 – 2.6 | 33 | 1.96±0.34 | 3.50±0.61 | 0.17±0.01 | 6.5±1.2 | 27.1±5.0 | 8.1±1.5 |
| 49-53 / 45-16 | 7 | 2.6 – 2.9 | 54 | 3.40±0.46 | 6.61±0.90 | 0.16±0.01 | 10.3±1.5 | 34.8±5.2 | 10.4±1.5 |
| 49-53 / 45-16 | 6 | 2.9 – 3.18 | 27 | 1.18±0.23 | 2.41±0.47 | 0.13±0.01 | 3.4±0.7 | 11.4±2.4 | 3.0±0.6 |
| 45-16 | 2 | ~4-7[e] | 1 | 0.11±0.11 | 0.20±0.30 | 0.14±0.01 | <0.4 | <1 | -- |
| commercial iron | 99 | background | 7 | 0.042±0.015 | -- | | | | |

[a] measured $^{60}$Fe/Fe ratios. The uncertainties from $^{60}$Fe denote statistical uncertainties only (1σ, using Poisson statistics).

[b] background & decay-corrected (d.c.) $^{60}$Fe/Fe-data. Surface and old layers are compatible with the measurement background obtained from chemistry blank samples. The age is based on the $^{26}$Al and $^{10}$Be data and tie-points of magnetic reversals.

[c] 'conc' means 'concentration'. Stable iron content of the leached material as measured via ICP-MS (averaged values, see Methods). The average leachable Fe content for the four cores was measured to 0.18% (core Eltanin 49-53), 0.25% (45-16), 0.3% (45-21) and 0.45% (50-02). The mean dry density of the sediments was 1.16·g·cm$^{-3}$.

[d] for sediments with 100% incorporation efficiency the Fe deposition equals the terrestrial fluence.

[e] uncertain by ~1 Myr.

**Table 2**

$^{60}$Fe/Fe-ratios from AMS measurements at ANU of layered samples of the two Pacific FeMn crust samples (Crust-1 and Crust-2) and of the two Atlantic FeMn nodules (no. 21 and 24).

| layer | depth (mm) | time period (Myr) | $^{60}$Fe counts detected | $^{60}$Fe/Fe ($10^{-15}$ at/at)[a] | $^{60}$Fe/Fe \|$_{d.c.}$ ($10^{-15}$ at/at)[b] | Fe conc. ($10^{-2}$ g g$^{-1}$)[c] | $^{60}$Fe conc. ($10^6$ at g$^{-1}$) | $^{60}$Fe incorp. rates (atoms·cm$^{-2}$·yr$^{-1}$) | $^{60}$Fe incorporation ($10^6$ at·cm$^{-2}$/layer) |
|---|---|---|---|---|---|---|---|---|---|
| **Crust-1** | | | | | | | | | |
| Layer 1 | 0 – 5 | 0 – 2.17 | 23 | 0.96±0.25 | 1.19±0.33 | 12.8±0.1 | 1.64±0.45 | 0.72±0.20 | 1.56±0.43 |
| Layer 2 | 5 – 10 | 2.17 – 4.35 | 74 | 1.58±0.23 | 3.60±0.55 | 11.8±0.1 | 4.56±0.68 | 2.00±0.30 | 4.34±0.65 |
| Layer 3 | 10 – 15 | 4.35 – 6.52 | 2 | 0.14±0.12 | 0.36±0.51 | 11.4±0.1 | 0.34±0.62 | 0.19±0.27 | 0.40±0.59 |
| Layer 4 | 15 – 20 | 6.52 – 8.70 | 26 | 0.38±0.09 | 2.49±0.97 | 13.7±0.2 | 3.67±1.43 | 1.61±0.63 | 3.49±1.36 |
| Layer 5 | 20 – 25 | 8.70 – 10.87 | 3 | 0.15±0.11 | 1.20±1.50 | 11.2±0.2 | 1.45±1.82 | 0.64±0.80 | 1.38±1.73 |
| **total** | | 0-4.35 & 6.52-8.70 | 123 | | -- | | | -- | **9.4±0.9** |
| **Crust-2** | | | | | | | | | |
| Layer 1-2 | 0 – 1.0 | 1.20 – 1.41 | 5 | 1.06±0.48 | 1.50±0.67 | 11.6±0.1 | 1.87±0.83 | 1.67±0.75 | 0.36±0.16 |
| Layer 3-5 | 1.0 – 2.5 | 1.41 – 1.73 | 37 | 1.28±0.21 | 2.01±0.33 | 11.9±0.1 | 2.60±0.43 | 2.33±0.38 | 0.74±0.12 |
| Layer 6-8 | 2.5 – 4.0 | 1.73 – 2.05 | 32 | 0.84±0.15 | 1.39±0.25 | 11.8±0.1 | 1.73±0.31 | 1.55±0.27 | 0.50±0.09 |
| Layer 9-10 | 4.0 – 5.8 | 2.05 – 3.05 | 20 | 0.55±0.12 | 1.09±0.24 | 11.1±0.1 | 1.35±0.30 | 0.46±0.10 | 0.46±0.10 |
| Layer 11-12 | 5.8 – 7.7 | 3.05 – 4.11 | 2 | 0.12±0.08 | 0.29±0.21 | 10.4±0.1 | 0.37±0.26 | 0.13±0.09 | 0.13±0.09 |
| Layer 13-26 | 7.7 – 21.0 | 4.11 –7 | 1 | <0.03 | <0.1 | 9 | <0.1 | <0.09 | <0.06 |
| **$^{60}$Fe:** | **0 – 7.7** | **1.20 – 3.05** | **94** | | -- | | | -- | **2.19±0.22** |
| **Nodule 21** | | | | | | | | | |
| Layer 1 | 0 – 3 | 0 – 1.8 | 3 | 0.16±0.11 | <0.23 | 15±2 | <0.4 | <0.13 | <0.23 |
| Layer 2 | 3 – 6 | 1.8 – 3.3 | 13 | 0.47±0.16 | 0.60±0.22 | 15±2 | 0.97±0.36 | 0.40±0.15 | 0.55±0.21 |
| Layer 3/4 | 6 –17 | 3.3 – 5.4 | 5 | 0.18±0.06 | <0.10 | 15±2 | <0.16 | <0.1 | <0.23 |
| **$^{60}$Fe:** | **3 – 6** | **1.8–3.3** | **13** | **0.47±0.16** | **0.60±0.22** | **15±2** | **0.97±0.36** | **0.40±0.15** | **0.55±0.21** |
| **Nodule 24** | | | | | | | | | |
| Layer 1 | 0 – 4 | 0–1.9 | 15 | 0.56±0.18 | 0.71±0.23 | 15±2 | 1.13±0.37 | 0.34±0.11 | 0.86±0.41 |
| Layer 2 | 4 – 8 | 1.9–3.3 | 5 | 0.23±0.12 | 0.45±0.23 | 15±2 | 0.71±0.37 | 0.27±0.15 | 0.54±0.34 |
| Layer 3/4 | 8 – 19 | 3.3–5.4 | 1 | 0.05±0.05 | <0.15 | 15±2 | <0.24 | <0.1 | <0.25 |

**Crust-1**

| layer | depth (mm) | time period (Myr) | $^{60}$Fe/Fe ($10^{-15}$ at/at)[a] | $^{60}$Fe counts detected | $^{60}$Fe/Fe $|_{d.c.}$ ($10^{-15}$ at/at)[b] | Fe conc. ($10^{-2}$ g g$^{-1}$)[c] | $^{60}$Fe conc. ($10^{6}$ at g$^{-1}$) | $^{60}$Fe incorp. rates (atoms·cm$^{-2}$·yr$^{-1}$) | $^{60}$Fe incorporation ($10^{6}$ at·cm$^{-2}$/ layer) |
|---|---|---|---|---|---|---|---|---|---|
| **$^{60}$Fe:** | **0 – 8** | **0–3.3** | 0.40±0.10 | **20** | **0.58±0.13** | 15±2 | **0.92±0.21** | **0.31±0.09** | **1.40±0.50** |

*a* measured $^{60}$Fe/Fe ratios. The uncertainties from $^{60}$Fe denote statistical uncertainties only (1σ, using Poisson statistics).

*b* background & decay corrected (d.c.) $^{60}$Fe/Fe data. The machine background of $^{60}$Fe/Fe=(0.042±0.015)×$10^{-15}$ was used for the subsequent background correction. Ages are based on the $^{10}$Be data and have an uncertainty of ±0.3 Myr (Crust-1) and ±0.5 Myr (Crust-2 and nodules).

*c* stable iron content of the dissolved crust material and of the leachate in case of the nodules, as measured via ICP-MS. The mean dry density of the crust and nodule samples was 1.9·g·cm$^{-3}$. 'conc.' means 'concentration'. The Fe concentration listed for Crust-2, layers 13-26 is the average; individual data range between 5.5 and 13.1%.

**Table 3**

Summary of $^{60}$Fe-deposition into various archives as obtained in this work and given in the literature[10,11,22] (no correction for incorporation efficiency). Uncertainties are 1σ.

| Deep-sea archive | cores | location | time period (Myr) | $^{60}$Fe detector events | $^{60}$Fe deposition ($10^6$ at·cm$^{-2}$)[a] |
|---|---|---|---|---|---|
| Sediment | 4 | Indian Ocean | 1.71 – 3.18 | 288 | 35.4±2.6 |
| FeMn Crust 1 | 2 | Pacific Ocean | 0 – 4.35 | 97 | 5.9±0.8 |
| FeMn Crust 1 | | | 6.52 – 8.70 | 26 | 3.5±1.0 |
| FeMn Crust 2 | | | 1.2 – 3.1 | 94 | 2.2±0.2 |
| FeMn nodules | 2 | Atlantic Ocean | 1.8 – 3.3<br>0 – 3.3 | 13<br>20 | 0.6±0.2<br>1.4±0.5 |
| FeMn Mona Pihoa[10] | 1 | Pacific ocean | 0 – 5.9 | 21 | ~9[b] |
| FeMn 237KD[11] | 1 | Pacific ocean | 1.74 – 2.61[b] | 69 | 1.5±0.4[b] |
| Lunar material[22] | 1 | Moon | integral | --[c] | ~10 |

[a] for Crust-1 and Crust-2 an incorporation efficiency of 17 and 7% respectively, has to be taken into account to calculate the $^{60}$Fe fluence from the deposition values; similarly 2 and 4% for the nodules.

[b] adjusted for a revised $^{60}$Fe and $^{10}$Be half-live values[7,8]

[c] not listed in Ref. 22.